Sensor-actuators

Microfluidic High-Power Electroosmotic Pumps Based on Glass Fiber Filters

Rafael Ecker* [ID], Tina Mitteramskogler* [ID], Andreas Fuchsluger* [ID], and Bernhard Jakoby** [ID]

Institute for Microelectronics and Microsensors, Johannes Kepler University Linz, 4040 Linz, Austria
*Graduate Student Member, IEEE
**Fellow, IEEE

Abstract—A surface phenomenon known as the electric double layer effect occurs in a few atomic layers at the fluid–solid interface. By applying an external electric field, this phenomenon is used to generate a fluidic flow, which is called electroosmosis, and the corresponding device electroosmotic pumps (EOPs). In order to immensely increase the fluid–solid contact surface and, consequently, the fluid volume that generates the desired fluidic flow, an EOP employing a glass fiber filter in the main channel is presented in this letter. As a result, our EOP can reach high pressures of up to 400 kPa as well as high flow rates up to the milliliter per minute range. The devised technology enables low-cost EOP fabrication by using a polymethyl methacrylate substrate and mostly thermal-based fabrication processes. In order to address the challenges associated with spurious gas generation due to electrolysis, this EOP uses ion conductive membranes to keep the unwanted electrolysis process outside of the channel. To endure highly aggressive chemical reactions, platinum wires are furthermore employed as electrodes in the EOPs.
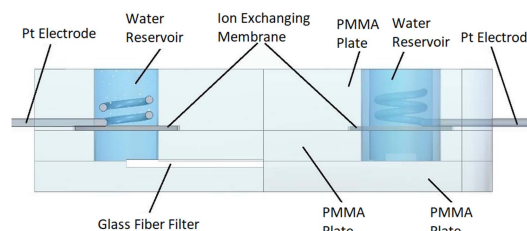
Index Terms—Sensor-actuators pump, glass fiber filter, high pressure, ion-exchanging membrane, polymeric substrate.

I. INTRODUCTION

Pumps are one of the essential parts of many microfluidics systems enabling the realization of miniaturized sensing platforms, where the pumps serve to move (most often water-based) fluids through the channels, thus enabling the system's intended functionality [1], [2], [3]. The key advantage of electroosmotic pumps (EOPs) is that they do not require moving components and provide pulse-free flow and pressure [4], [5]. As a result, it is simple to reduce the size of the EOPs and integrate them, e.g., into lab-on-a-chip systems [6], [7] or use them, e.g., for microflow injection analysis or microelectronic cooling [8]. Microfluidics is a broad subject, and as such, there is a demand for microfluidic pumps in a variety of fields, including research, chemical analysis, medicine, biology, and mixing applications [9], [10], [11], [12], [13].

Any liquid–solid contact exhibits an interfacial effect known as the electric double layer phenomenon. At a solid–liquid interface, most solid surfaces are negatively charged and consequently lead to a positively charged liquid area near the interface, typically only a few atomic layers thick [14]. The total charge depends on the material combination and is described by the so-called zeta potential. If now an external electric field is applied parallel to such a contact surface (i.e., along the channel axis in case of a microfluidic channel), a force will act on the charged particles, and consequently, liquid starts to flow, which is the so-called electroosmotic effect. It can be used in EOPs, since the flowing charged layers at the channel walls entrain the liquid in the channel, thus creating a flow. A comprehensive overview of electroosmotic flow is provided in [15].

Utilizing self-fabricated frits represents a common concept of increasing the contact surface between the liquid–solid interface accordingly boosting the electroosmotic effect [5], [16], [17]. To enable a cost efficient fabrication, the technology presented in this letter uses commercially available low-cost glass fiber filters to fulfill this task [18]. Furthermore, the combination of glass and water features a rather high zeta potential, which allows our pump to run at high pressures and flow rates. The zeta potential of some other EOPs [5], [19], [20] is increased by adding water supplements; however, the output of the EOP presented here is achieved with pure distilled water.

To obtain a low-cost fabrication process without the need of costly machinery, we utilize heat- and solvent-based bonding methods, polymeric substrates, and commercially accessible components.

Early attempts related to this technology have been presented earlier [3] and have been enhanced to finally achieve the process described here. In particular, a novel polymethyl methacrylate (PMMA) bonding method to achieve a stronger, deformation-free, and optical immaculate boding is used enabling the pump to endure higher pressures. The described bonding technique is particularly intended to be used for the development and integration of sensors and sensors–actuator systems into polymer-based microfluidic chips. The EOP itself has undergone significant remodeling and is now equipped with an ion-exchanging membrane. This makes it possible to relocate the platinum electrodes outside of the main channel of the EOP, which fixes the issues resulting from accumulation of gases in the channels caused by spurious electrolysis at the electrodes. Furthermore, the possible pressure could be increased by the factor of four now enabling to draw water from a reservoir at the pump's input. In order to facilitate the long-term operation of the EOPs, the revised configuration also degasses distilled water in the input reservoir.

Using the presented technology, our EOP can achieve higher flow rates (up to 300 µL/min, and even more is possible by adapting the channel geometry) and higher pressures (400 kPa) than other EOPs
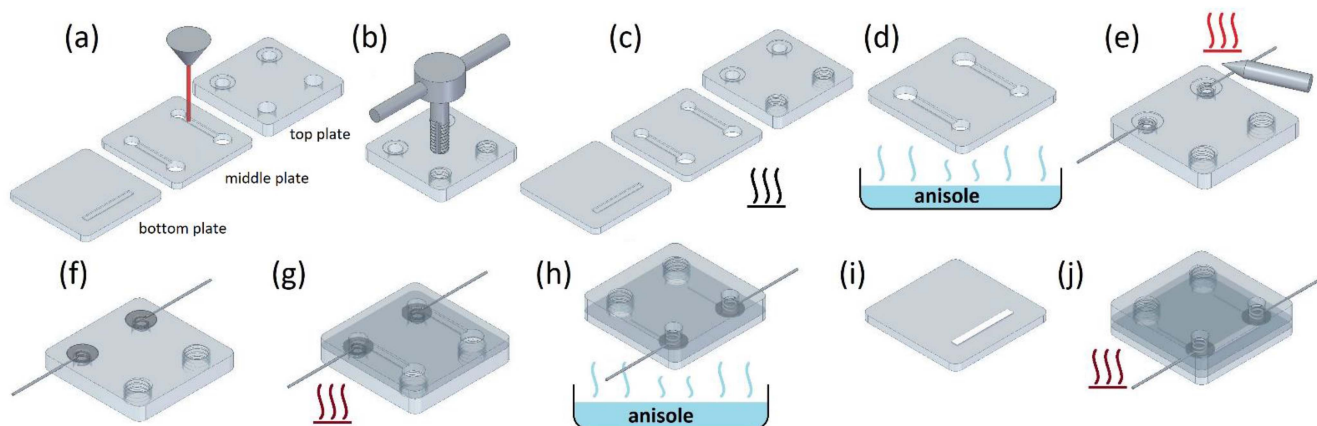
Fig. 1. Fabrication process of the EOP with ion-exchanging membrane. (a) Laser engraving of the channel structures and laser cutting. (b) Thread cutting for later Luer fittings. (c) Annealing process to avoid stress cracks. (d) Solvent treatment in anisole vapor to enable a strong bonding afterward. (e) Bending and fixing of the platinum wires used as electrodes. (f) Placing of the ion-exchanging membranes. (g) Thermal bonding process. (h) Solvent treatment in anisole vapor to enable a strong bonding afterward. (i) Placing of the laser cut glass fiber filter. (j) Thermal bonding process.

[1], [2], [5], [17], [19], [20], [21], [22], which is also facilitated by the fact that our device is suitable for operation with comparatively high voltages.

II. EXPERIMENTAL SECTION

A. Fabrication Process

The devised fabrication process is depicted in Fig. 1. Commercially available PMMA plates (Röhm GmbH, Germany) with a thickness of 4 mm for the top plate and 1.5 mm for the bottom and middle plates were employed as substrate for the EOP. Using a laser cutting/engraving machine (Speedy 300 flexx, Trotec Laser GmbH, Austria), the channel structures are laser engraved into PMMA substrates and laser cut in the first step [see Fig. 1(a)]. Threads are cut into the proper holes, as shown in Fig. 1(b), to facilitate the connection of the input and output using Luer fittings later on. An annealing phase is required [see Fig. 1(c)] to reduce the risk of stress-induced cracks. To do so, the plates are heated up for at least 1 h to 75 °C. The oven is then turned OFF, and the plates are left inside until they reach room temperature. A newly developed bonding method that combines solvent and heat bonding to provide a strong link between the PMMA plates is introduced. First, magnets are used to fix at least one component—in our example, the center part—to the glass cap of a petri dish. Next, anisole is poured into the lower section of the petri dish, which is then sealed with a cover with the PMMA plate on it [see Fig. 1(d)]. The solvent is now just a few millimeters away from the plate's later contact surface. According to tests, the PMMA plates should be treated in anisole vapor for 45 to 50 min. A shorter treatment period results in poorer bonding quality, whereas a much longer treatment period causes the channel architecture to distort due to the beginning dissolution of the PMMA surface. Meanwhile, as shown in Fig. 1(e), two 0.25-mm diameter platinum wires are bent into a spiral form and then melted into the top plate using a soldering iron. Subsequently, laser-cut N115 ion-exchanging membranes (Nafion, Chemours, USA) are positioned on the upper plate [see Fig. 1(f)]. The middle plate is immediately put onto the top plate when its treatment period has ended. The plates are finally bonded together using a thermal bonding procedure. A heat press (CR2042-1, LTQ Vapor) that has been preheated to 85 °C and applies a pressure of 1000 kPa (at the bonding interface) for 20 min is
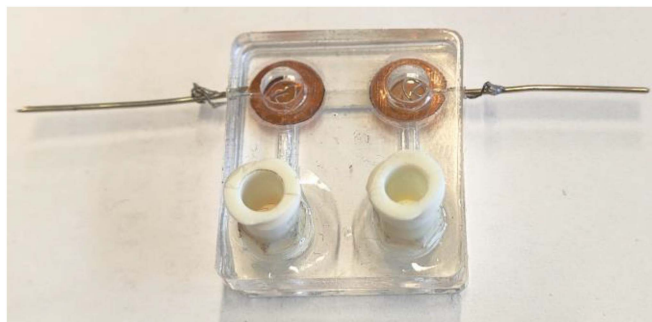

Fig. 2. Fabricated EOP with ion-exchanging membranes.

utilized to this end. The stack of the middle and top plates is flipped and placed into the previously mentioned anisole vapor treatment process after it has cooled down to room temperature [see Fig. 1(h)]. A laser-cut glass fiber filter (Grade 259, Camlab, U.K.) piece is then inserted into the main channel of the bottom plate [see Fig. 1(i)]. Subsequently [see Fig. 1(j)], the bottom plate is attached to the previously bonded plates using the same thermal bonding procedure. The thinner platinum wires are soldered to a thicker (0.91-mm-diameter) tinned copper wire that is fixed to the EOP's side walls in order to facilitate an easy connection. Finally, Luer fittings are inserted into the thread, and if needed (they may leak at a pressure above 200 kPa), sealed by being adhered to the pump with epoxy resin. Fig. 2 depicts an image of a fabricated EOP.

B. Measurement Setup

A pump is characterized by measuring the output flow rate at different output pressures. To perform this measurement, it is necessary to build a setup, which enables the measurement of both actual flow rate and pressure.

A sketch of the used setup is shown in Fig. 3. As a flow sensor [see Fig. 3(b)], a Sensirion SLI-1000 or a Sensirion SLI-430 (for zero pressure flow rates below 100 μL/min) is used. As a pressure sensor [see Fig. 3(f)], for pressures up to 200 kPa, an ABPMANV030PG2A3 sensor, and for larger pressures, an ABPMANV150PG2A3 sensor by Honeywell are used. Both the flow and pressure sensors are connected
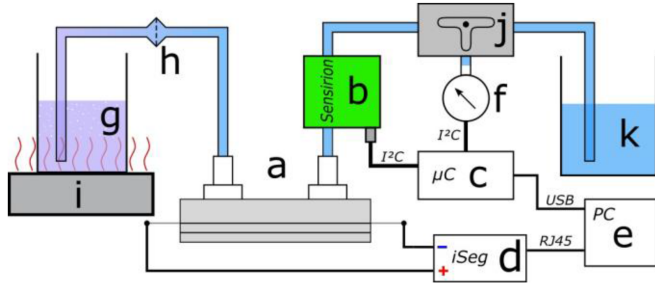
Fig. 3. Measurement setup. (a) EOP. (b) Flow sensor. (c) Micro-controller. (d) High-voltage power supply. (e) Computer. (f) Pressure sensor. (g) Input reservoirs. (h) Filter. (i) Hot plate. (j) Three-way valve. (k) Output reservoirs.

to a microcontroller [Arduino Nano, Fig. 3(c)] by an I²C bus. The microcontroller evaluates the measurement data, displays them on a liquid crystal display, and sends them to a PC [see Fig. 3(e)]. The EOP [see Fig. 3(a)] is powered by a high-voltage power supply [SHR, iseg Spezialelektronik GmbH, Germany, Fig. 3(d)], which also sends measurement data to the PC. With increasing temperature, the ability of water to dissolve gas decreases [23]. The majority of the applied energy from the power source is transformed into heat, particularly in the main channel (the glass fiber filter). As a result, water is heated there, which causes gas to fall out into the channel causing potential obstruction. The performance of the EOP begins to decrease, and if the channel is entirely blocked, the EOP stops functioning. In order to reduce this effect, water in the input reservoir [see Fig. 3(g)] is degassed before entering the pump by heating it to 95 °C on a hot plate [see Fig. 3(i)].

C. Measurement Procedure

After inserting the EOP into the sample holder and connecting it to the power source and the water tubes, the pump is filled with degassed deionized (DI) water. To this end, three-way valves and syringes inserted into the input and output tubes are utilized. In addition, DI water needs to be added to the small water reservoirs located on the top of the EOP, where the platinum electrodes terminate. During operation, water in these reservoirs will be converted into hydrogen on the one side and into oxygen on the other side. Hence, it is necessary to refill them regularly. Upon completion of these preparations, the EOP is operational.

The pump is connected to water reservoirs at its inputs and outputs, where the reservoirs are connected to perform the desired flow rate over pressure measurements, thus avoiding pressure differences due to variations in the water level. After switching on the high-voltage power supply, the flow rate starts to increase. After a few seconds, the EOP reaches a reasonably steady flow rate at zero pressure Q_0. Following the closure of the three-way valve, the flow rate decreases, and the pressure begins to rise. Air remaining in the tube to the pressure's sensors becomes compressed, and the silicone tubes starts to expand. The maximum pressure p_{max} is reached when the flow rate is approaching zero. At this point, the valve is opened again, and the measurement is stopped.

III. EXPERIMENTAL RESULTS

In this section, we present the achieved output characteristics of the EOP and discuss the limitations of the demonstrator device.

Table 1. Measurement Data for EOPs With Different Channel Dimensions

channel dimensions		measurement data		
l (mm)	w (mm)	V (kV)	Q_0 (μl/min)	p_{max} (kPa)
9	1	0,5	35	76
		1	83	149
		1,5	131	225
		2	95	308 [a]
		2,5	157	313 [a]
9	2	0,5	44	12
		1	85	19
		1,5	144	39
		2	204	61
		2,5	245	74
		3	320	134 [a]
14	2	0,5	28	81
		1	74	128
		1,5	85	209
		2	156	267 [a]
14	1	0,5	13	52
		1	35	98
		1,5	47	184
		2	67	322
		2,5	79	323 [a]
		3	90	412 [a]

[a] at high pressure the water in the channel of the EOP starts to boil. Given is the maximum measured pressure.
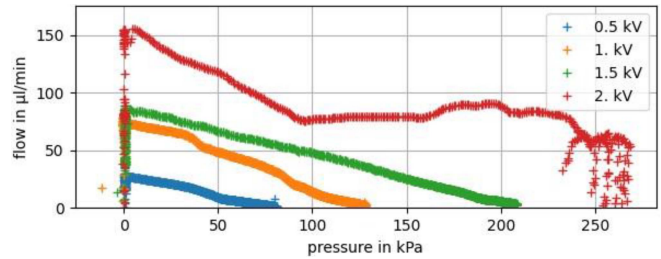

Fig. 4. Output characteristics of a sample EOP with channel dimensions of length $l = 14$ mm and width $w = 2$ mm at different voltages. The red 2-kV curve gets to the thermal limit at 250 kPa.

A. Measurement

To demonstrate the functionality of our EOP technology and designs, EOPs with different channel dimensions (width w and length l) are fabricated and measured at different voltages V using the measurement procedure described earlier. In Table 1, the measurement data of different sample pumps are collected.

In Fig. 4, the output characteristics of one EOP at various voltages are shown. The characterization of different EOPs showed that a wider channel leads to a higher flow rate at a constant voltage, while the achievable maximum pressure decreases. Increasing the channel length leads to higher possible pressures and to a reduction of the flow rate. Adapting the design parameters, it is, thus, possible to fabricate the EOP, which fits the user's requirements.

B. Limitations

While the devised and fabricated EOPs operate at remarkable flow rates and pressures, at the moment, the thermal power dissipation is

the limiting factor preventing the further increase of the attainable pressures and flow rates. A few watts of thermal energy have to be dissipated at the high applied voltages. Water becomes warm, thus when flowing, eliminating the heat by means of convection. But the heat transport due to convection is much less efficient at high output pressures because of the low maximum possible flow rates there. The heat then has to be mainly transported through the PMMA plates, but PMMA is a poor heat conductor. Hence, water becomes hotter, which, depending on the application, may represent a limit of this approach.

IV. CONCLUSION AND OUTLOOK

In this letter, the fabrication and the functionality of EOPs for high flow rate (up to the milliliter per minute range) and high pressure (up to 400 kPa) are presented and validated using water as working liquid. A glass fiber filter placed into the main channel immensely increases the contact surface between water and solid and, hence, the area where the electroosmotic effect is present. To fabricate the EOPs, a newly introduced bonding process, combining solvent and thermal bonding, for PMMA is used. This enables a leak-free operation even at high output pressures in the order of 400 kPa. The improved bonding process is considered to be generally utilizable for polymer-based devices and, thus, also other microfluidic chip designs. With the use of an ion-exchanging membrane, the spurious electrolysis process is shifted outside of the EOP avoiding gas-related blockage. Furthermore, it is also possible to draw in water at the input port. By changing the polarity of the supply voltage, the flow direction can be easily reversed.

As next steps, EOPs featuring a broader array of channel dimensions shall allow to identify limits of possible flow rate and pressures associated with the current design. Investigations will target possibilities to improve the thermal dissipation, using cooling techniques and materials with better thermal conductivity.

ACKNOWLEDGMENT

REFERENCES

[1] J. Sun et al., "A mobile and self-powered micro-flow pump based on triboelectricity driven electroosmosis," *Adv. Mater.*, vol. 33, no. 34, 2021, Art. no. 2102765, doi: 10.1002/adma.202102765.

[2] Z. Ye, R. Zhang, M. Gao, Z. Deng, and L. Gui, "Development of a high flow rate 3-D electroosmotic flow pump," *Micromachines*, vol. 10, no. 2, 2019, Art. no. 112, doi: 10.3390/mi10020112.

[3] R. Ecker, A. Fuchsluger, and B. Jakoby, "Electroosmotic pump using a glass fiber filter for high flow rate water transport," in *Proc. IEEE SENSORS Conf.*, 2021, pp. 1–4, doi: 10.1109/SENSORS47087.2021.9639725.

[4] Q. Li, P. Zhang, Z. Ye, H. Zhang, X. Sun, and L. Gui, "A liquid metal based, integrated parallel electroosmotic micropump cluster drive system," *Lab Chip*, vol. 24, no. 4, pp. 896–903, 2024, doi: 10.1039/D3LC00926B.

[5] J. A. Tripp, F. Svec, J. M. J. Fréchet, S. Zeng, J. C. Mikkelsen, and J. G. Santiago, "High-pressure electroosmotic pumps based on porous polymer monoliths," *Sens. Actuators B, Chem.*, vol. 99, no. 1, pp. 66–73, 2004, doi: 10.1016/j.snb.2003.10.031.

[6] M. K. D. Manshadi, D. Khojasteh, M. Mohammadi, and R. Kamali, "Electroosmotic micropump for lab-on-a-chip biomedical applications," *Int. J. Numer. Model.: Electron. Netw., Devices Fields*, vol. 29, no. 5, pp. 845–858, 2016, doi: 10.1002/jnm.2149.

[7] M. Gao and L. Gui, "A handy liquid metal based electroosmotic flow pump," *Lab Chip*, vol. 14, no. 11, pp. 1866–1872, 2014, doi: 10.1039/C4LC00111G.

[8] X. Wang, C. Cheng, S. Wang, and S. Liu, "Electroosmotic pumps and their applications in microfluidic systems," *Microfluidics Nanofluidics*, vol. 6, no. 2, pp. 145–162, 2009, doi: 10.1007/s10404-008-0399-9.

[9] G. Kaur, M. Tomar, and V. Gupta, "Development of a microfluidic electrochemical biosensor: Prospect for point-of-care cholesterol monitoring," *Sens. Actuators B, Chem.*, vol. 261, pp. 460–466, 2018, doi: 10.1016/j.snb.2018.01.144.

[10] V. L. Kopparthy and E. J. Guilbeau, "Highly sensitive microfluidic chip sensor for biochemical detection," *IEEE Sens. J.*, vol. 17, no. 20, pp. 6510–6514, Oct. 2017, doi: 10.1109/JSEN.2017.2746419.

[11] N. Zhang, K. Zha, and J. Wang, "Exploring the design efficiency of random microfluidic mixers," *IEEE Access*, vol. 9, pp. 9864–9872, 2021, doi: 10.1109/ACCESS.2021.3050161.

[12] P. Agnihotri, "Analysis of interfacial mixing zone and mixing index in microfluidic channels," *Microfluidics Nanofluidics*, vol. 27, no. 2, 2023, Art. no. 12, doi: 10.1007/s10404-022-02618-z.

[13] R. Ecker, T. Mitteramskogler, M. Langwiesner, A. Fuchsluger, M. A. Hintermüller, and B. Jakoby, "A self-sealing modular microfluidic system using PDMS blocks with magnetic connections," *IEEE Access*, vol. 11, pp. 82882–82893, 2023, doi: 10.1109/ACCESS.2023.3302327.

[14] Y. Luo, J. Qin, and B. Lin, "Methods for pumping fluids on biomedical lab-on-a-chip," *Front. Biosci.*, vol. 14, no. 10, pp. 3913–3924, 2009, doi: 10.2741/3500.

[15] R.-J. Yang, L.-M. Fu, and Y.-C. Lin, "Electroosmotic flow in microchannels," *J. Colloid Interface Sci.*, vol. 239, no. 1, pp. 98–105, 2001, doi: 10.1006/jcis.2001.7551.

[16] A. Brask, J. P. Kutter, and H. Bruus, "Long-term stable electroosmotic pump with ion exchange membranes," *Lab Chip*, vol. 5, no. 7, pp. 730–738, 2005, doi: 10.1039/B503626G.

[17] S. Zeng, C.-H. Chen, J. C. Mikkelsen, and J. G. Santiago, "Fabrication and characterization of electroosmotic micropumps," *Sens. Actuators B: Chem.*, vol. 79, no. 2, pp. 107–114, 2001, doi: 10.1016/S0925-4005(01)00855-3.

[18] T. J. O'Shaughnessy and B. J. Johnson, "Optimized electroosmotic materials for water transport," in *Proc. Chem. Biol. Defense Phys. Sci. Technol. Conf.*, 2008.

[19] S. Liu, Q. Pu, and J. J. Lu, "Electric field-decoupled electroosmotic pump for microfluidic devices," *J. Chromatography A*, vol. 1013, no. 1, pp. 57–64, Sep. 2003, doi: 10.1016/S0021-9673(03)00941-5.

[20] L. Chen, H. Wang, J. Ma, C. Wang, and Y. Guan, "Fabrication and characterization of a multi-stage electroosmotic pump for liquid delivery," *Sens. Actuators B, Chem.*, vol. 104, no. 1, pp. 117–123, 2005, doi: 10.1016/j.snb.2004.05.013.

[21] Q. Yang et al., "Multilayer track-etched membrane-based electroosmotic pump for drug delivery," *Electrophoresis*, vol. 45, pp. 433–441, 2024, doi: 10.1002/elps.202300213.

[22] V. Silverio, P. A. G. Canane, T. A. Martins, R. Afonso, S. Cardoso, and E. Batista, "Development of a microfluidic electroosmosis pump on a chip for steady and continuous fluid delivery," *Biomed. Eng.*, vol. 68, no. 1, pp. 79–90, 2023, doi: 10.1515/bmt-2022-0051.

[23] R. Battino and H. L. Clever, "The solubility of gases in liquids," *Chem. Rev.*, vol. 66, no. 4, pp. 395–463, 1966.